DOI: 10.1002/cmdc.200700216

Generation of Carrier Peptides for the Delivery of Nucleic Acid Drugs in Primary Cells

Robert Rennert,[a] Ines Neundorf,[a] Heinz-Georg Jahnke,[b] Philipp Suchowerskyj,[c] Pascal Dournaud,[d] Andrea Robitzki,[b] and Annette G. Beck-Sickinger*[a]

Now that the human genome has been decoded, the demand for novel therapeutic concepts, such as gene and stem cell therapy, is higher than ever before. Although new and better pharmaceutical agents are available, their efficient delivery to the intracellular site of action is still a serious challenge. A possible solution to this problem is the use of cell-penetrating peptides as delivery vectors, including derivatives of human calcitonin (hCT). The aim of this study was to synthesise novel branched hCT-derived peptides for the noncovalent delivery of nucleic acids. The uptake of the resulting oligocationic peptides into various cell lines as well as primary cells was monitored by fluorescence microscopy. To determine the appropriate peptide–plasmid charge ratios for efficient cell transfection, electromobility shift assays were carried out. Finally, flow cytometric and fluorescence microscopic studies of gene expression highlighted two novel hCT-derived peptides as highly effective in the delivery of noncovalently complexed plasmid DNA. Thus, the absence of cytotoxicity paired with highly efficient cell internalisation and transfection rates, in primary cells as well, make both peptides powerful candidates as drug delivery vectors, especially for plasmid DNA, for both in vivo and ex vivo therapeutic applications.

Introduction

In the current age of the decoded human genome, stem cell[1] and gene therapies,[2] DNA vaccination,[3,4] and RNA interference[5–7] have become increasingly interesting approaches for the control and treatment of a broad range of diseases. Because of their hydrophilic nature, however, these macromolecules require novel delivery concepts. In vivo therapies require safe and efficient carrier systems, whereas ex vivo gene delivery into cells might be an appropriate approach for hematopoietic cells or stem cell therapy, for example.[8] Such a strategy would allow a more careful treatment of the patient, as the in vitro preparation of the cells would allow monitoring of the effects prior to application in vivo. Furthermore, ex vivo targeting of the desired cells is more promising than in vivo targeting, in which bioavailability and bioactivity are serious problems for many reasons.[9]

Unfortunately, a crucial prerequisite for such pharmaceutical applications is effective cellular nucleic acid delivery. This process has been investigated for decades, primarily to generate a powerful research tool for elucidating gene structure, metabolic regulation, and function. However, there are currently no safe and effective systems available. The most frequently used delivery systems for DNA or RNA these days are viruses. They are perfectly suited to effect cellular delivery of DNA or RNA: they are highly cell-target selective, they are very effective at nucleic acid translocation across biological membranes, they have the capacity to bypass or escape endocytotic pathways, they are efficient at intracellular nucleic acid release, and they have high nuclear targeting and expression rates (due to strong promoters and enhancers). Owing to these excellent properties, viral DNA and RNA delivery systems have seen widespread application in basic research and clinical settings.[10,11]

Nevertheless, serious drawbacks of viral carriers include toxicity and immunogenicity.[12] These problems can be solved by using physical transfection methods such as microinjection, particle bombardment,[13] and electroporation[14] (which are more or less restricted to in vitro applications), or synthetic nonviral delivery systems (which also allow in vivo application). The general principle of the latter approaches is based on the formation of complexes between positively charged molecules and negatively charged nucleic acids. Well-known examples for such chemical methods are based on calcium phosphate,[15] cationic lipids,[16,17] polyethyleneimine (PEI),[18] and cell-penetrating peptides. However, the transfection efficiencies of the

[a] *R. Rennert, Dr. I. Neundorf, Prof. Dr. A. G. Beck-Sickinger*
Institute of Biochemistry
Faculty of Biosciences, Pharmacy and Psychology
Leipzig University, Brüderstr. 34, 04103 Leipzig (Germany)
Fax: (+49) 341-97-36909
E-mail: beck-sickinger@uni-leipzig.de

[b] *H.-G. Jahnke, Prof. Dr. A. Robitzki*
Centre for Biotechnology and Biomedicine
Institute of Biochemistry
Faculty of Biosciences, Pharmacy and Psychology
Leipzig University, Deutscher Platz 5, 04103 Leipzig (Germany)

[c] *P. Suchowerskyj*
University Hospital for Children and Adolescents
Leipzig University, Oststr. 21/25, 04103 Leipzig (Germany)

[d] *Dr. P. Dournaud*
INSERM U676, Hôpital Robert-Debré
Université Paris 7 Denis-Diderot
48 Boulevard Sérurier, 75019 Paris (France)

synthetic transfection systems in current use are not as high as those of viral systems. This is also the case for the so-called cell-penetrating peptides, a very heterogeneous class of peptides that share the capacity to traverse biological membranes and shuttle various cargoes inside cells.[19,20]

Cell-penetrating and carrier properties have also been described for peptides derived from human calcitonin (hCT), a 32-residue peptide amide that is secreted by the thyroid gland and involved in the regulation of calcium balance. It was found to possess membrane-translocating abilities, as nasal therapeutic application is as effective as i.v. injection.[21] Structure–activity studies have shown that the C-terminal fragment hCT(9–32) still permeates cellular membranes even if the calcitonin receptor-activating N-terminal region (amino acids 1–8) of hCT is missing. Therefore, hormone side effects are not expected.[22,23] The truncated derivative hCT(9–32) was shown to efficiently shuttle the anticancer drug daunorubicin into various cell lines.[24] Furthermore, the transport of proteins has been shown by using a covalently linked 27-kDa green fluorescent protein (GFP).[25] Recently, a branched hCT(9–32) derivative was used to successfully transfect the neuroblastoma cell line SK-N-MC.[26] This peptide was shown to be internalised into the cells via a 'lipid-raft'-dependent, endocytotic pathway.[27] We are currently looking for derivatives of human calcitonin as nonviral delivery systems for DNA and RNA.

The aim of the work presented herein was the synthesis of novel branched hCT-derived peptides with markedly improved cell internalisation and cell transfection efficiencies. By using these new carrier peptides, we have been able to shuttle vector DNA very effectively into HEK 293 and SK-N-MC cells, and also into primary neurons and embryonic chicken cardiomyocytes. Furthermore, we investigated the influence of the charge ratio in peptide–plasmid complex formation, and the effects of plasmid quantity, incubation time, and the application of the antimalarial drug chloroquine (CQ) on peptide-mediated transfection efficiencies. Two highly effective branched peptides representing a new generation of hCT-derived carrier peptides are presented herein. Both of them expand the application of carrier peptides to nucleic acid delivery, especially in differentiated primary cells, toward potential application in ex vivo stem cell therapy.

Results

Peptide synthesis

The synthesis of the peptides was performed by both automated and manual solid-phase peptide synthesis (SPPS) using the Fmoc–*t*Bu strategy. The peptides were alternatively N-terminally labelled with carboxyfluorescein (CF) at the hCT fragment. For the later branched peptides, the hydroxy group of CF was protected with a triphenylmethyl (trityl) group to avoid any side reaction during synthesis. To introduce the side chains at position 18 into the branched peptides, the N^{ε} atom of Lys18 was protected with Dde. When the synthesis and CF labelling of the hCT fragment were completed, this ε-amino group was selectively deprotected with hydrazine. Subsequently, the Lys-rich side sequence was introduced in a second automated SPPS. Finally, all acid-labile protecting groups, including the trityl group of CF, were removed, and the peptides were cleaved from the resin with TFA. The peptides were purified by preparative RP-HPLC and analysed by MALDI-ToF mass spectrometry and analytical RP-HPLC. Peptide sequences, molecular weights, and net charges are listed in Table 1.

Cell viability after peptide treatment

To avoid undesirable cytotoxic effects during cell transfection, all peptides and transfection agents, that is, the plasmid and CQ, were examined for cytotoxic effects on HEK 293 cells using a fluorimetric resazurin-based cell viability assay. After treatment of sub-confluent HEK 293 cells with up to 150 μM peptide solution for 24 h, cell viability was found to be >95% for every peptide. Furthermore, to ensure a gentle procedure for cell transfection, samples containing 0.5 μg plasmid DNA and

Table 1. Peptide amino acid sequences, molecular masses, and net charges of the investigated peptides.

Peptide	Sequence[a]	$M_{W\,calcd}$ [Da][b]	$M_{W\,exptl}$ [Da]	Net Charge[c]
hCT(9–32)	LGTYTQDFNKFHTFPQTAIGVGAP–NH_2	2610.0	2610.1	+1
hCT(9–32)-br	LGTYTQDFNKFHTFPQTAIGVGAP–NH_2 PKKKRKVEDP*GVGFA*┘	4246.0	4245.7	+4
hCT(9–32)-2br	LGTYTQDFNKFHTFPQTAIGVGAP–NH_2 PKKKRKVEDP*GVGFA*PKKKRKVEDP*GVGFA*┘	5886.8	5886.9	+7
hCT(18–32)-2br	KFHTFPQTAIGVGAP–NH_2 PKKKRKVEDP*GVGFA*PKKKRKVEDP*GVGFA*┘	4845.8	4845.5	+8
hCT(18–32)-k7	KFHTFPQTAIGVGAP–NH_2 KKRKAPKKKRKFA┘	3165.9	3166.0	+11
2br	PKKKRKVEDP*GVGFA*PKKKRKVEDP*GVGFA*–NH_2	3292.3	3292.1	+7
k7	KKRKAPKKKRKFA–NH_2	1613.1	1613.0	+10
Tat(48–60)	GRKKRRQRRRPPQ–NH_2	1717.1	1717.5	+9

[a] Underlined: NLS derived from SV40 large T antigen; italics: cleavage sites for cathepsin B. All peptides were synthesised as C-terminal amides. [b] For internalisation studies, all peptides were N-terminally labelled with CF as well (M_W + 356.4 Da). [c] Peptide net charge at physiological pH.

up to 150 μM CQ were tested after incubation for 6 h as well; no cytotoxicity was observed.

As reference, we investigated the effect of polyethyleneimine (PEI)–plasmid complexes on cell viability. PEI is often used as a nonviral vector for transient cell transfections. However, a major drawback of this agent is its severe cytotoxicity. By using branched 25-kDa PEI, a PEI nitrogen/DNA phosphate ratio of 20:1 was described to be a good compromise between cytotoxicity and transfection efficiency.[18] Therefore, we tested the toxic effects of PEI–DNA complexes on HEK 293 cells, with N/P ratios of up to 20:1 over an incubation period of 4 h. Ratios of 20:1 and 10:1 caused severe cytotoxicity with ~6% of viable cells (data not shown). An N/P ratio of 5:1 showed a HEK 293 cell viability of 59%, whereas a ratio of 1:1 showed no cytotoxicity in the resazurin-based assay. However, the cell morphology in the latter case was affected, as observed by microscopy and flow cytometry (data not shown). The effects of peptide solutions (150 μM for 24 h), CQ plus DNA (150 μM for 6 h), and PEI–DNA complexes (5:1 ratio, 4 h) on cell viability are shown in Figure 1.

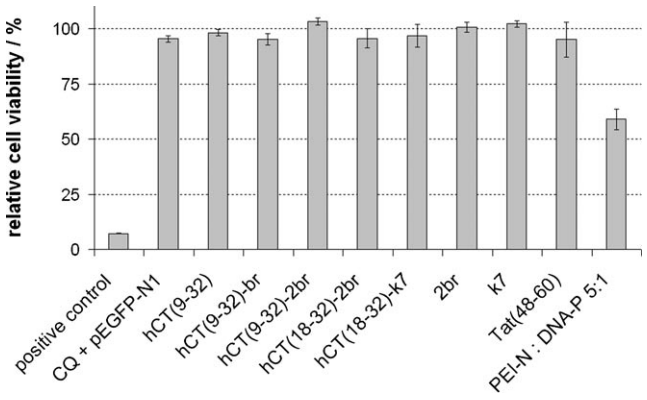

Figure 1. Relative viability of HEK 293 cells after treatment with peptide solution (150 μM) for 24 h, chloroquine (150 μM) with pEGFP-N1 (0.5 μg) for 6 h (CQ + pEGFP-N1), and polyethyleneimine–plasmid complex (PEI–DNA N/P = 5:1) for 4 h. Cell viability was determined by using a fluorimetric resazurin-based cell viability assay. Cells incubated with 70% alcohol for 10 min served as positive control for cytotoxicity. Data are normalised to untreated cells (100% viability). Chloroquine and the vector DNA pEGFP-N1 were used for transfection experiments, and thereby, incubated not longer than the tested 6 h.

Cellular peptide uptake

The carboxyfluorescein-labelled branched peptides CF-hCT(9–32)-2br and CF-hCT(18–32)-k7 were efficiently internalised in a broad collection of cell lines and primary cells, as visualised by fluorescence and confocal microscopy after incubation for 1 h at 37 °C (Figure 2). Hence, both are very potent cell-penetrating peptides. The cellular uptake of CF-hCT(9–32), CF-hCT(9–32)-br, both side chain sequences CF-2br and CF-k7, as well as CF-Tat(48–60) as control peptides were also investigated (data not shown). These data indicate a distinct increase in uptake efficacy of both of the novel branched hCT derivatives relative to the unbranched and nearly uncharged CF-hCT(9–32) as well as to CF-hCT(9–32)-br. Thereby, the efficacy of peptide uptake was similar to that of CF-Tat(48–60). However, in contrast to CF-2br, which showed no significant cellular uptake, the peptide CF-k7 was effectively internalised.

In Figure 2, a punctuated fluorescence pattern of CF-hCT(9–32)-2br and CF-hCT(18–32)-k7 is shown, which indicates localisation of the internalised peptides within discrete vesicular compartments in the cytoplasm. This is the case in all cell lines studied, such as HEK 293, SK-N-MC, HeLa, MCF-7, and COS-7 as well as in primary chicken cardiomyocytes and rat hippocampal neurons, and suggests an endocytotic pathway of peptide internalisation. Untreated cells as well as cells incubated with the fluorescent marker CF itself were studied in parallel for control. However, in both cases no intracellular fluorescence was observed (data not shown).

Electromobility shift assay (EMSA)

To evaluate the potential of these new peptides to effect complete DNA complexation, and to determine optimal peptide–DNA ratios, we performed EMSA studies. In principle, as peptide molecules shield the negative charges of the DNA upon complex formation, the electrophoretic migration rate of the DNA is decreased relative to DNA alone, hence the mobility shift. If all negative charges are neutralised by the basic peptide residues, the mobility shift is maximised, and the DNA remains in the loading pocket of the gel. In contrast, a lower retardation of the complex migration in the gel reflects a greater number of unshielded negative charges as a result of only partial nucleotide complexation by the peptide. For the EMSA, peptide and plasmid were complexed for 1 h under the same conditions as for cell transfections. Four different peptide–plasmid charge ratios were analysed. Subsequently, the complexes were run on an agarose gel, and the DNA was visualised by ethidium bromide (EtBr) staining.

Whereas the branched hCT-derived peptide hCT(18–32)-k7 as well as the reference peptides k7 and Tat(48–60) showed a complete band shift to the loading pocket even at the smallest peptide–plasmid charge ratio of 5:1, the complex with hCT(9–32)-2br was fully shifted at a charge ratio of 30:1. This indicates a required complete complexation and coating of the DNA by these peptides at a ratio of at most 30:1. The peptides hCT(9–32)-br, hCT(18–32)-2br, and the reference peptide 2br were not able to complex the plasmid completely, even at the highest charge ratio (60:1). These results are shown in Figure 3. Because a peptide–plasmid charge ratio of 30:1 was considered to be a good compromise between complete DNA complexation and economic reasons, this ratio was used in the following cell transfection experiments.

Degradation patterns

Degradation experiments were performed to evaluate the metabolic stability of the branched peptides hCT(9–32)-2br and hCT(18–32)-k7. The parent peptide hCT(9–32) was also tested as a reference. Because the molecular integrity of a carrier peptide is assumed to influence its delivery efficiency,[28] metabolic studies should help to clarify reasons for the observed trans-

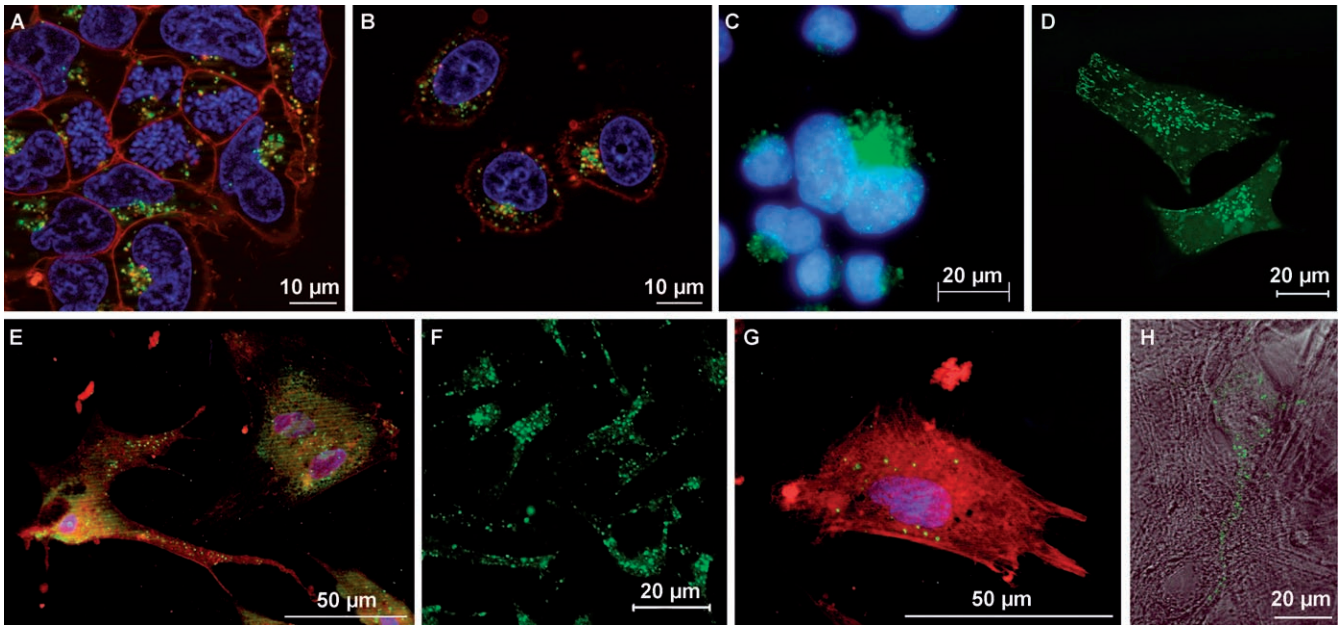

Figure 2. Cellular uptake of CF-hCT(18–32)-k7 (A–E) and CF-hCT(9–32)-2br (F–H). CF-hCT(18–32)-k7 was efficiently internalised in A) HEK 293, B) MCF-7, C) COS-7, D) HeLa, and E) primary chicken cardiomyocytes. For CF-hCT(9–32)-2br, cellular uptake is shown in F) HeLa, G) primary chicken cardiomyocytes, and H) primary rat hippocampal neurons. Cells were incubated for 1 h with 5 μM (H), 25 μM (A–C), and 50 μM (D–G) peptide solution. In some cases, the nucleus was counter-stained with H33342; cells in panels A) and B) were stained with transferrin–Texas Red for clathrin-dependent endocytosis, and those shown in panels E) and G) were immune histologically stained against α-actinin with Cy3. Images were taken using either fluorescence (A–C, E, G) or confocal (D, F, H) microscopy; scale bars are indicated.

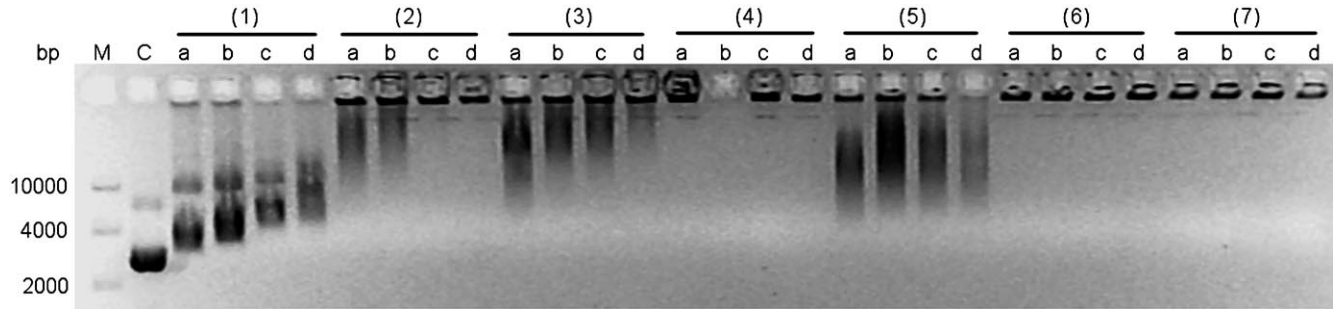

Figure 3. Electromobility shift assay (EMSA) of noncovalent complexes of pECFP-N1 (4.7 kb) and the peptides. The expression vector pECFP-N1 (0.25 μg) was complexed in four various peptide–plasmid charge ratios (a, 5:1; b, 15:1; c, 30:1; d, 60:1) for 1 h at 37 °C in aqueous solution with: (1) hCT(9–32)-br, (2) hCT(9–32)-2br, (3) hCT(18–32)-2br, (4) hCT(18–32)-k7, (5) 2br, (6) k7, or (7) HIV-Tat(48–60). Samples were separated in a 1% agarose gel and stained with EtBr. M: 1-kb DNA ladder, C: control with 0.5 μg pure plasmid.

fection rates. To analyse metabolites that arise, the peptides were incubated with human blood serum for up to 240 h and fractionated by RP-HPLC. Because the peaks were detected by CF fluorescence, only the N-terminal fragments containing the CF label were analysed. The collected peak fractions were further identified by MALDI-ToF mass spectrometry. The suggested cleavage sites of hCT(9–32) and both branched peptides are summarised in Figure 4.

For hCT(9–32), cleavage sites were detected after positions Tyr 12, Thr 13, His 20, Ala 26, and Ala 31 after 48 h. This is in good agreement with recently published degradation patterns of this peptide and its stabilised analogues in heparinised blood plasma.[29] In this study, metabolic instabilities after Tyr 12, Thr 13, and Ala 26 in hCT(9–32) and after His 20 in several D-phenylalanine- and *N*-methylphenylalanine-modified analogues could be confirmed as well. Degradation after Ala 31 was not observed, but could be explained by carboxypeptidase activity.

The branched peptide hCT(9–32)-2br showed metabolic degradation within the hCT fragment next to position Thr 13 after 48 h as well, but only to a minor degree. Furthermore, the C terminus of the hCT fragment seemed to be stabilised by the oligocationic side sequence, as there was no further cleavage site. Interestingly, the side sequence 2br was also quite stable. After serum incubation for 48 h, the sequence was cleaved after positions Lys 17′ and Arg 20′, apparently by trypsin-like enzymes. In contrast, hCT(18–32)-k7 was strongly degraded after just 24 h. Cleavage sites after Lys 18, Pro 23, and

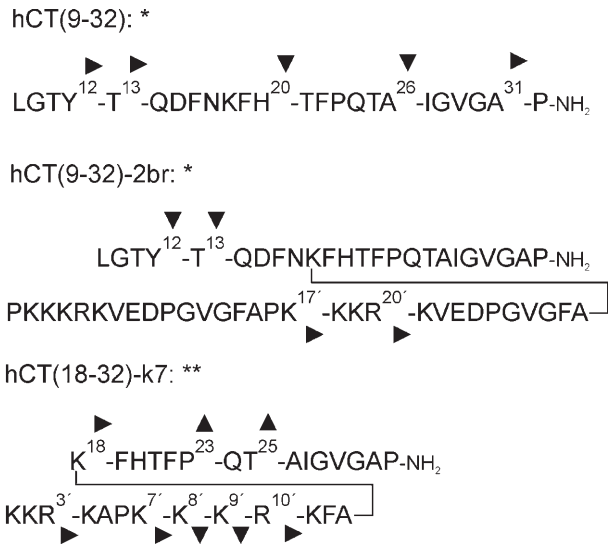

Figure 4. Suggested metabolic cleavage sites of CF-labelled hCT analogues after incubation for 24 (**) and 48 h (*) in human blood serum. The orientations of the triangles indicate the amount of detected metabolites as analysed by RP-HPLC peak intensity: ▲ > ► > ▼. Numbers without primes denote amino acid positions in the hCT fragment, whereas numbers with primes correspond to positions within the oligocationic side chain sequences.

Thr25 were observed within the core fragment hCT(18–32). Furthermore, the Lys- and Arg-rich side chain sequence k7 was the object of intense proteolytic degradation, with cleavage after most of the basic amino acid positions.

Circular dichroism

The conformations of all hCT-derived peptides and the two separate side chain fragments 2br and k7 were investigated by circular dichroism (CD) in aqueous phosphate buffer (10 mM, pH 7.0) as well as in a solution of 50% TFE. CF-labelled peptides were analysed for spectroscopic standardisation of the peptide solutions.

In phosphate buffer, all peptides revealed random coiled structures with minima around 199 nm. In contrast, in the presence of TFE, the peptides hCT(9–32), hCT(9–32)-br, hCT(9–32)-2br, hCT(18–32)-2br, and 2br adopt a more α-helical conformation. However, with the exception of hCT(9–32), its typical α-helical spectra is in good agreement with published data,[29] all spectra have a slight hypsochromic shift. The two negative bands are located between 201–204 and 221–225 nm; the positive peaks are between 190–193 nm. The side chain fragment k7 and hCT(18–32)-k7 retain the random coiled conformation (data not shown).

To determine if the noncovalent DNA complex affects the conformation of the carrier peptides, CD was performed on DNA complexes with hCT(9–32)-2br, hCT(18–32)-2br, and hCT-(18–32)-k7. Peptide–plasmid complex formation was carried out as described above, and CD data were subsequently measured in aqueous phosphate buffer. For normalisation, the spectrum of a solution of pure DNA was subtracted. As shown in Figure 5, all three peptides revealed a random coiled structure with minima between 196–199 nm in complex with vector DNA as well. Whereas the spectra of free and noncomplexed hCT(18–32)-2br are virtually congruent, for the other two peptides, the minima of the peptide–plasmid complexes are slightly hypsochromically shifted, relative to the free peptides (3 nm for hCT(9–32)-2br, and 2 nm for hCT(18–32)-k7).

Cell transfection

To test the novel branched hCT-derived cell-penetrating peptides for their ability to transfect eukaryotic cells effectively with vector DNA, in vitro studies were carried out with the human embryonic kidney cell line HEK 293 and the human neuroblastoma cell line SK-N-MC, as well as freshly isolated primary chicken cardiomyocytes and rat hippocampal neurons in serum-free media.

The transfection rate and fluorescence protein expression (of eGFP, eCFP, and eYFP) was studied by fluorescence microscopy and flow cytometry, respectively. For reference, cells were transfected with Lipofectamine 2000, a highly efficient commercial liposomal transfection agent. The transfection rates determined by flow cytometry were normalised to the Lipofectamine 2000 rate, which was set 100%. In addition to the branched hCT analogues, the side chain sequences 2br and k7 were analysed, as well as the well-described Tat(48–60). As negative controls, untreated cells, cells incubated with plasmid DNA alone, and cells treated with DNA and CQ were investi-

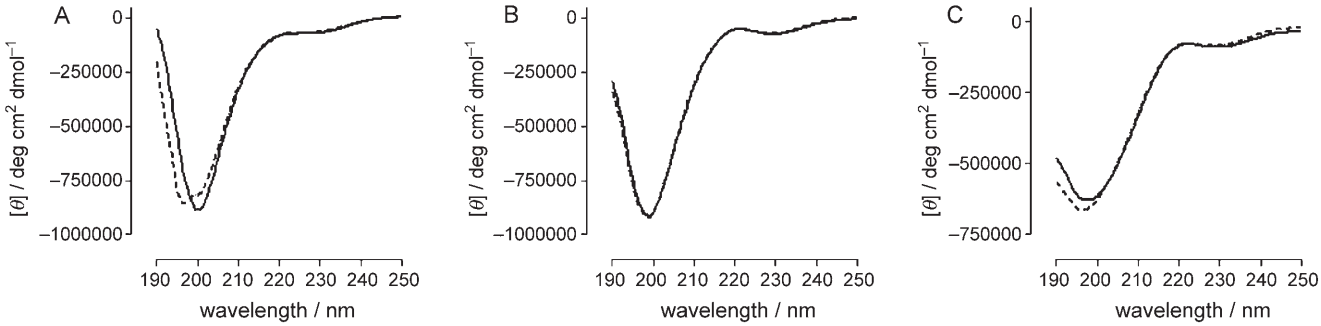

Figure 5. CD spectra of the CF-labelled branched hCT-derived peptides (10 μM). The peptides A) CF-hCT(9–32)-2br, B) CF-hCT(18–32)-2br, and C) CF-hCT(18–32)-k7 were measured both free (——) and in complex with vector DNA pEGFP-N1 at a charge ratio of 30:1 (-----) in aqueous phosphate buffer (10 mM, pH 7.1).

gated. However, cell transfection was not observed with any of these approaches (data not shown).

As shown in Figure 6, the branched peptides hCT(9–32)-2br and hCT(18–32)-k7 acted as potent transfection agents, but the transfection rates were highly dependent on the investigated cell line. While HEK 293 cells were quite easy to transfect (68% transfected cells with Lipofectamine 2000), SK-N-MC cell transfection was more difficult. Moreover, with Lipofectamine 2000 only ~6% of these cells were transfected. In principle, the same was found for the peptidic carriers. Considering the absolute quantity of peptide-mediated transfected cells, HEK 293 cells were transfected much more effectively than the neuroblastoma cells SK-N-MC.

As previous studies have suggested, one prerequisite for efficient peptide-mediated intracellular cargo transport is the addition of agents such as chloroquine.[30] Indeed, this is in full agreement with the data presented herein. Efficient cell transfection required the application of this weak and membrane-permeable base. For HEK 293 transfection, CQ concentrations up to 125 μM in the transfection mixture were tested. The transfection rate increased with increasing CQ concentration in the range of 0–125 μM (data not shown). However, because high concentrations of CQ are cytotoxic, CQ at 125 μM was assumed to be a good compromise between transfection yield and the potential cytotoxic effects of CQ.

The peptide–plasmid charge ratio and the incubation time showed a direct impact on the transfection rate as well. As established by flow cytometric studies, a peptide–plasmid charge ratio of 30:1 for DNA complexation permitted good transfections. In the case of hCT(9–32)-2br the transfection efficiency for HEK 293 cells was found to increase by a factor ~6 with a charge ratio of 30:1 instead of 15:1 (19 versus 3% transfection of all cells). With hCT(18–32)-k7 the increase was less significant (12 versus 9% transfection of all cells). These results are supported by the EMSA studies. However, a charge ratio of 60:1 did not further increase the transfection rates significantly (data not shown). Therefore, we did not use charge ratios higher than 30:1 for further studies.

Incubation of the cells with the peptide–plasmid complexes was tested for 2, 3, and 4 h, resulting in good transfection rates after 4 h. Incubation times of >4 h showed, in some cases, slightly increased transfection rates. However, because with prolonged incubation the risk of cytotoxic effects from CQ is increased as well, we generally used an incubation time of 4 h. In contrast, an increase in plasmid quantity from 0.5 to 1.5 μg did not cause any distinct improvement (data not shown). Hence, for practical and economic reasons, the plasmid amount was set at 0.5 μg for the 96-well plate format, and a 30:1 peptide–plasmid charge ratio was used in combination with 4 h incubation.

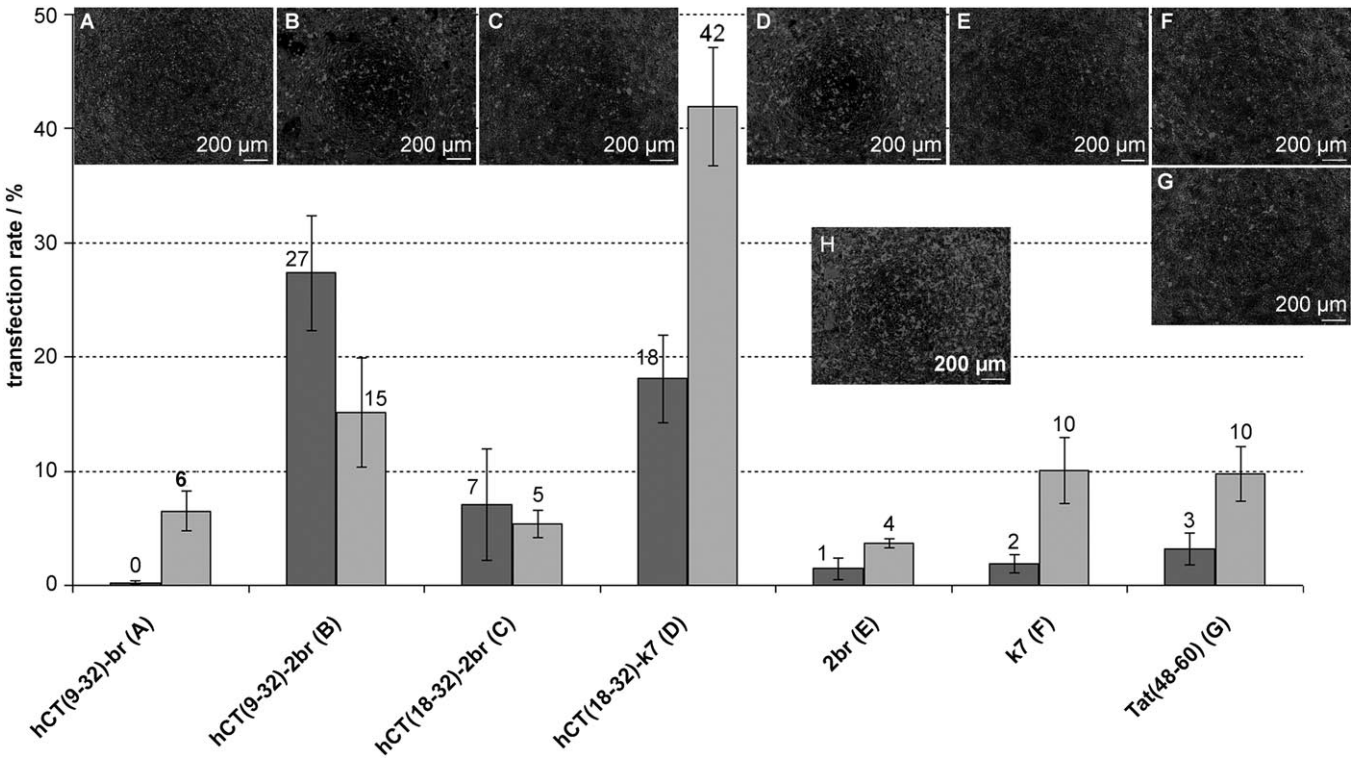

Figure 6. Rates of peptide-mediated cell transfection were determined by flow cytometric studies and normalised to the transfection rates obtained with Lipofectamine 2000. Vector DNA pEYFP-N1 was noncovalently complexed with the peptides in a peptide–plasmid charge ratio of 30:1 at 37 °C for 1 h. Cells were pre-incubated with 125 μM CQ in serum-free medium for 1 h. HEK 293 (dark grey) and SK-N-MC cells (grey) were incubated with peptide–plasmid complexes and CQ for 4 h. Expression was measured after 24 h. Fluorescence microscopic images of the transfected HEK 293 cells support the flow cytometric data. Images were taken immediately before flow cytometric studies: A) hCT(9–32)-br, B) hCT(9–32)-2br, C) hCT(18–32)-2br, D) hCT(18–32)-k7, E) 2br, F) k7, and G) Tat(48–60). As reference, cells were transfected with Lipofectamine 2000 without CQ (H).

Interestingly, whereas hCT(9–32)-2br was the most potent peptide for transfecting HEK 293 cells (~27% transfected relative to Lipofectamine 2000), hCT(18–32)-k7 was by far the best peptide (~42% relative to Lipofectamine 2000) for SK-N-MC cell transfection. Surprisingly, the closely related branched peptide hCT(18–32)-2br failed to transfect either cell line effectively. The same was observed for hCT(9–32)-br as well as for 2br, k7, and even for Tat(48–60). The latter two peptides showed some transfection of SK-N-MC cells, but approximately fourfold less than hCT(18–32)-k7. Fluorescence images confirmed the quantitative flow cytometric data (exemplified on HEK 293 cells in Figure 6). Interestingly, considering the peptide's decreased net positive charge, the transfection efficiency was not affected if N-terminally CF-labelled peptides were used as delivery vectors (Figure 7).

Flow cytometric data on SK-N-MC cells suggested increased fluorescence protein expression levels compared to cells treated with Lipofectamine 2000, when transfected with hCT(9–32)-2br and hCT(18–32)-k7. In both cases, the expressed fluorescence level was ~1.5-fold higher than with Lipofectamine 2000 or Tat(48–60) (data not shown). One possible explanation is the association of the DNA with the branched hCT-derived peptides in larger complexes, which may translocate a greater number of plasmids into a given cell. This could result in higher expression levels in transfected cells, but for the same reason, a lower observed transfection rate.

To analyse the potential of these novel branched peptides to shuttle nucleic acids into cells more closely related to in vivo systems, peptide-mediated transfection was investigated on primary chicken cardiomyocytes and on primary rat hippocampal neurons by fluorescence microscopy. The images clearly show the high potential of both hCT(9–32)-2br and hCT(18–32)-k7 as cell transfection agents (Figure 8). By using hCT(9–32)-2br, the peptide-mediated transfection rate of rat hippocampal neurons was ~1/4 of that obtained with Lipofectamine 2000. This is in good agreement with results obtained with primary chicken cardiomyocytes. However, with these cells, the best transfection efficiencies were observed for hCT(18–32)-k7 (~19% transfected cells relative to Lipofectamine 2000). By using hCT(9–32)-2br, the normalised transfection rate was 13%, but with Lipofectamine 2000 as well, only 6–7% of all cardiomyocytes were transfected. This underscores the big challenge in transfecting primary cells.

Discussion

Efficient cell transfection, that is, the intracellular administration of nucleic acids, is one prerequisite for the successful application of DNA and RNA molecules in clinical therapies. In general, nucleic acid delivery systems can be roughly categorised into two groups: viral vector-mediated and nonviral vector-mediated systems.[28,31] Highly evolved components still make viral systems the by far most effective means of nucleic acids delivery, providing both highly efficient delivery and strong gene expression.[32] However, some serious drawbacks of these systems cannot be overlooked. In particular, cytotoxicity and immunogenicity hamper the applicability of viral systems in clinical protocols and basic research.[33]

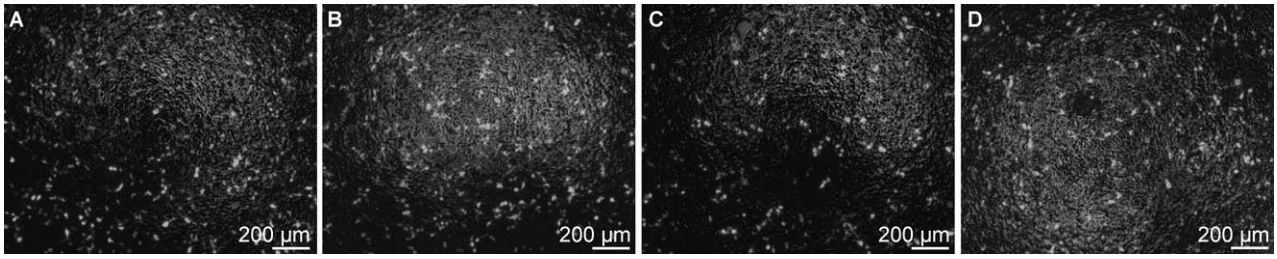

Figure 7. Fluorescence microscopic images of HEK 293 cells transfected with hCT(9–32)-2br and hCT(18–32)-k7 with and without N-terminal CF label: A) hCT(9–32)-2br, B) CF-hCT(9–32)-2br, C) hCT(18–32)-k7, and D) CF-hCT(18–32)-k7. Cells were incubated for 4 h with the noncovalent peptide–pECFP-N1 complexes (peptide–plasmid charge ratio of 30:1) in the presence of 125 μM CQ. Peptide–plasmid complexation was performed for 1 h. Images were taken after 24 h ECFP expression.

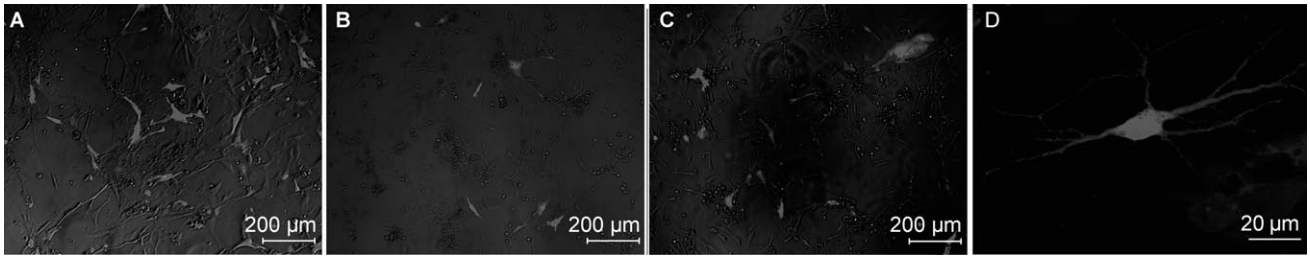

Figure 8. Fluorescence microscopic images of A–C) transfected primary chicken cardiomyocytes, and D) primary rat hippocampal neurons. Cells were incubated for 4 h with the noncovalent peptide–pEGFP-N1 complexes (peptide–plasmid charge ratio of 30:1) in the presence of 125 μM CQ (for the hippocampal neurons (D) ratio = 20:1, with 75 μM CQ). Peptide–plasmid complexation was performed for 1 h with hCT(9–32)-2br (B and D), and hCT(18–32)-k7 (C). As reference, cells were transfected with Lipofectamine 2000 without CQ (A). Images were taken after 24 h EGFP expression; scale bars are indicated.

Owing to these disadvantages, the development of effective nonviral transfection reagents remains a challenge. Except for some physical transfection methods, the majority of nonviral systems are based on synthetic molecules. These synthetic systems combine the ease of handling, defined molecular structures, automated synthesis, and precise analytical characterisation.[9,12,28]

Carrier peptides share these advantages. These cell-penetrating peptides are able to import themselves and cargoes as diverse as plasmid DNA,[34–37] oligonucleotides,[38,39] small interfering RNA (siRNA),[40,41] peptide nucleic acids (PNAs),[42] proteins,[25,43,44] and nanoparticles.[45]

Because cell penetration and carrier peptide properties have also been described for peptides derived from hCT, the truncated and branched hCT peptide hCT(9–32)-br was previously synthesised and found to successfully transfect the neuroblastoma cell line SK-N-MC.[26] However, because hCT(9–32)-br failed to offer satisfactory transfections of other cell lines, the goal was the optimisation of hCT-derived carrier peptides. This was realised by combining the cell-penetrating ability of the calcitonin fragment hCT(9–32) and a truncated version hCT-(18–32), as well as an improved cationic character of the nucleic acid binding moiety. In this process, we maintained the branched structure to avoid steric hindrance between the hCT fragment and the cationic side chain. Indeed, several studies have indicated that a branched peptide design improves the efficiency of peptide-mediated gene delivery.[46,47] However, these carrier peptides must overcome several problems for effective DNA and RNA delivery; these include: 1) efficient noncovalent complexation of the negatively charged nucleic acid, 2) mediation of a powerful interaction between the carrier complex and the cellular membrane, 3) preferably efficient escape from endocytotic compartments, and 4) targeting of the shuttled nucleic acids to the nucleus.[9,12,28]

It was our goal to synthesise novel branched hCT-derived peptides capable of overcoming these barriers while in a noncovalent complex with a nucleic acid cargo. In parallel, we used the well-established oligocationic carrier peptide HIV-1 Tat(48–60) as a reference. Numerous studies have attested to the high cellular uptake rates of Tat(48–60) and related analogues.[48–50] The potential of a C-terminally Cys-modified Tat-(48–60) to efficiently translocate covalently coupled DNA into cells was shown by Sandgren and co-workers.[37]

To aim for at least three of the above-mentioned prerequisites for effective nucleic acid delivery, a large number of positive charges was shown to be advantageous.[9] To address this, it is beneficial to link a nuclear localisation sequence (NLS), rich in Lys and Arg residues, to the carrier peptide.[51] For instance, the peptidic carriers MPG and Pep-1 are chimeric molecules that contain the NLS of SV40 large T antigen. Both peptides were shown to efficiently deliver nucleic acids as well as noncovalently linked peptides and proteins into cells.[41,52,53] For this purpose, the peptides hCT(9–32)-2br and hCT(18–32)-2br were equipped with the side chain sequence 2br, which consists of two SV40-derived NLSs. To strive for the same goal, but with a smaller peptide, the truncated k7 side chain sequence was introduced in hCT(18–32)-k7 as a variant of 2br. Hence, with net charges of +7, +8, and +11 at physiological pH, hCT-(9–32)-2br, hCT(18–32)-2br, and hCT(18–32)-k7, respectively, should be able to effect strong complex formation with nucleic acids. Furthermore, because the initial contact between the peptide–cargo complex and the cell might be an electrostatic interaction between free redundant basic residues of the carrier and anionic components of the extracellular plasma membrane surface (e.g. cell-surface proteoglycans[9,37]), a high positive net charge for the whole peptide–DNA complex should improve the cellular uptake as well. Therefore, a prerequisite for effective cell transfection should be the complete shielding of all negative DNA charges by the carrier peptide. Moreover, to provide a sufficient number of positive charges for a proper complex–membrane interaction, an excess of positive peptidic charges is crucial for plasmid complexation. However, as indicated by our EMSA studies, it is not adequate to consider the pure net charge of the peptides alone. Indeed, as observed for hCT(9–32)-2br (+7), hCT(18–32)-k7 (+11), k7 (+10), and Tat-(48–60) (+9), the peptide net charge nicely correlates with the peptide–plasmid charge ratio required to effect complete DNA packaging. In our studies, a peptide/plasmid ratio of 30:1 was sufficient for complete DNA complexation. Increasing the ratio to 60:1 did not increase the transfection efficiency of hCT(9–32)-2br or hCT(18–32)-k7 significantly. Furthermore, the peptides are present in large excess. Considering the good transfection rates of both latter peptides under these conditions, however, it may be that the redundant, noncomplexed peptides help to initiate the endocytotic machinery.

Nevertheless, as observed for hCT(18–32)-2br (+8) and 2br (+7), even a high positive net charge cannot guarantee sufficient coverage of the cargo, even with peptide in great excess. We found that this effect has a direct impact on the transfection efficiency of the peptides. No peptide with incomplete DNA complexation was able to transfect cells convincingly. In addition, it can be assumed that incomplete complexation protects the DNA less effectively from nuclease activity when the complex enters the cell. Recently, Kleemann et al. designed a Tat-derived DNA carrier and demonstrated its protective role against hydrolytic degradation by cationic complex formation.[35] Interestingly, the ability of the peptides to completely complex DNA at moderate peptide–plasmid ratios correlates directly with their cellular uptake efficiencies as free peptides. As indicated by fluorescence and confocal fluorescence microscopy hCT(9–32)-2br, hCT(18–32)-k7, the side chain sequence k7 itself, and the reference peptide Tat(48–60) internalise as free peptides with good rates in a number of different cell lines. This is probably due to enhanced membrane association mediated by the 7–11 positive net charges of these peptides.

However, despite their efficient DNA complexation and cell penetration, both Tat(48–60) and peptide k7 failed to transfect the cells as effectively as hCT(9–32)-2br and hCT(18–32)-k7. Thus, the high basic residue content alone cannot explain the powerful transfection ability of these peptides. It is conceivable that the branched peptide design combined with the optimal length of the side chain sequences 2br and k7 separates both the nucleic acid binding moiety and the cell-penetrating peptide fragments hCT(9–32) and hCT(18–32), respectively. The

finding that the side chain sequence 2br itself is neither effectively taken up by the cells nor able to transfect cells to more than a minor degree, indicates that the hCT fragment hCT(9–32) is still the driving force of peptide and complex internalisation. In the case of hCT(18–32)-k7, the side sequence k7, which internalises as the free peptide at good rates, might compensate for the decreased cellular entry of the truncated fragment hCT(18–32).[54] In fact, the peptide uptake rates of hCT(18–32)-k7 are even better than those determined for hCT(9–32)-2br. The transfection capacities are similar, however, in that they are dependent on the cell type. The failure of the sequence k7 alone in transfecting cells efficiently with DNA supports the assumption that a branched peptide design, with two spatially separated moieties for nucleic acid complexation and cell membrane penetration, increases the efficiency due to less steric hindrance and better spatial orientation. Moreover, CD studies indicate a rather small conformational change of the branched hCT-derived peptides during plasmid complexation. The same was observed in CD studies by Deshayes et al. of the carrier peptide Pep-1, but in complex with a cargo peptide.[55] Because the hCT peptides do not appear to be strongly affected by DNA binding, the effective cell penetration in conjunction with the smart design of both hCT(9–32)-2br and hCT(18–32)-k7 might explain their good transfection rates. In the case of the free carrier peptides, the α-helical conformation of hCT-(9–32)-2br detected in the presence of TFE is in good agreement with the strong amphipathic α-helical character of hCT-(9–32) that was observed when the peptide interacted with several model membranes.[56–58] These interactions were limited to the lipid head groups. However, such a shallow localisation of the peptide is clearly sufficient to alter membrane organisation, and therefore, to give the signal for endocytotic uptake. In this context noncomplexed peptides may play an important role in triggering this endocytotic mechanism.

The metabolic stability of a delivery vector is assumed to have an impact on its delivery efficiency as well. On one hand, maintaining the molecular integrity of the carrier as it enters the target cell is one prerequisite for efficient cargo delivery, but on the other hand, it is likely that metabolic degradation of the carrier, to a certain extent, is important for intracellular cargo release and might prevent local or systemic toxicity as well.[28] Therefore, we investigated the proteolytic degradation of both branched analogues hCT(9–32)-2br and hCT(18–32)-k7 as well as of hCT(9–32) in human blood serum. The degradation patterns of hCT(9–32) is in good agreement with published data.[29,59] Interestingly, the branched peptide hCT(9–32)-2br was more stable; the core fragment hCT(9–32) was cleaved to only a minor extent around Thr13, whereas the Lys-rich side chain was digested at only two positions in a trypsin-like degradation. Apparently, the additional 2br sequence and the branched peptide design protect the core fragment hCT(9–32) efficiently against metabolic degradation, probably because of steric hindrance of proteolytic enzymes and molecular shielding. Therefore, because hCT(9–32)-2br offers good transfection rates, the advantage of high metabolic stability seems to compensate for a likely hampered cargo release. In contrast, the smaller and more basic side sequence of hCT(18–32)-k7 is much more sensitive to trypsin-like enzymes, as the sequence k7 was virtual completely degraded within 24 h. Thus, its protective effect on the core hCT(18–32) is limited. In contrast to hCT(9–32)-2br, a hCT(18–32)-k7–DNA complex might be more susceptible to proteolytic enzymes until the target cell is reached, but once internalised, cargo release might be more efficient. However, it is important to keep in mind that the transported cargo may affect carrier peptide stability as well, due to steric hindrance of proteolytic enzymes, for example. Therefore, the metabolic stability of the peptides in complex with the DNA cargo is an appropriate subject for continued investigations.

In fact, the third prerequisite for effective nucleic acid delivery, the efficient escape of the cargo from endocytotic compartments,[9,12,28] has not been achieved by hCT(9–32)-2br and hCT(18–32)-k7 per se. As described previously, both peptides require the application of a supporting agent such as CQ for suitable transfection and expression rates. The enhancing effect on gene expression after endocytotic cell transfection mediated by the weak, membrane-permeable base CQ was previously described by Erbacher and colleagues.[30] It is thought to protect the endocytotically internalised nucleic acids from intracellular degradation through neutralisation of the acidic compartments, decreasing endosomal delivery to lysosomes, and destabilising the complex between carrier peptide and cargo.[60] Erbacher et al. detected this complex dissociation in the presence of >20 mM CQ, a concentration described to be easily reached inside endocytotic vesicles of HepG2 cells. Indeed, both transfection rates and expression levels increased proportionally with CQ concentration (up to 125 μM). The best results were obtained with cells pre-treated with CQ for at least 1 h.

The final challenge for successfully internalised DNA is its nuclear targeting. Because viral NLSs fused to synthetic delivery vectors have been shown to support DNA transport inside the nucleus,[61] the NLS derived from SV40 large T antigen should provide hCT(9–32)-2br with this feature. However, hCT-(18–32)-k7 proves that the complete NLS is not necessary. One possible explanation is that positively charged regions of the carrier complex could serve as signals for nuclear localisation. However, the precise mechanism of how the DNA translocates into the nucleus is still unknown for most of the synthetic carrier systems. Another possibility for nuclear entry of the DNA could be an association with chromatin upon breakdown of the nuclear envelope during mitosis. Such a process was observed for some cationic lipid and polymer-mediated delivery systems (see [9] for references). This might be the reason behind the cell-cycle dependence of gene transfer with many delivery vectors.[62] In fact, the best transfection efficiencies were obtained by using the novel branched hCT peptides with sub-confluent proliferating cells. Furthermore, mitosis-dependent nuclear translocation may explain the rather limited transfection efficiency in primary cells by nonviral DNA delivery methods.[63] Indeed, with the hCT-derived carrier peptides, the lower transfection efficiency with primary cells seems to be caused by a decrease in the number of very efficiently transfected cells, which is probably due to a smaller number of di-

viding cells in the primary culture. Nevertheless, both novel branched hCT-derived carrier peptides have proven their high potential to transfect primary cells as well (hCT(9–32)-2br for rat hippocampal neurons, and hCT(18–32)-k7 especially for chicken cardiomyocytes).

In conclusion, hCT(9–32)-2br and hCT(18–32)-k7 represent the successful synthesis of two novel branched hCT-derived carrier peptides that are optimised for the noncovalent delivery of DNA and RNA. Supported by chloroquine, both peptides mediated transfections with good rates and strong gene expression in several cell lines as well as in primary cells. For all cases, transfection rates and expression levels were significantly higher than those observed with the noncovalently linked reference peptide Tat(48–60). Furthermore, as the capacity to cross the membranes of all tested cell types was considerably improved by the addition of the side chain sequences 2br and k7, both peptides represent a new generation of hCT-derived carrier peptides. Owing to their high uptake rates and lack of cytotoxicity, hCT(9–32)-2br and hCT(18–32)-k7 are promising delivery vectors for cargo of any kind. Therefore, both peptides could serve as tools for novel therapeutic concepts, such as ex vivo preparation in stem cell therapy. We are currently investigating their application as noncovalent shuttles for aptamers and siRNA.

Experimental Section

Materials

N^{α}-Fmoc-protected amino acids were purchased from IRIS Biotech (Marktredwitz, Germany). 1-Hydroxybenzotriazole (HOBt) and 4-(2′,4′-dimethoxyphenyl-Fmoc-aminomethyl)phenoxy (Rink amide) resin were obtained from NovaBiochem (Läufelfingen, Switzerland). Diisopropylcarbodiimide (DIC), the resazurin-based in vitro toxicology assay kit, ethidium bromide (EtBr), paraformaldehyde, and 25-kDa branched polyethyleneimine were purchased from Sigma–Aldrich (Taufkirchen, Germany). Trifluoroacetic acid (TFA, peptide synthesis grade) was obtained from Riedel-de Haën (Seelze, Germany). *O*-(7-Azabenzotriazol-1-yl)-1,1,3,3-tetramethyluronium hexafluorophosphate (HATU), *N*,*N*-diisopropylethylamine (DIEA), thioanisole, *p*-thiocresole, piperidine, ethanedithiole, trifluoroacetic acid (HPLC grade), Trypan blue, 5(6)-carboxyfluorescein (CF), chloroquine (CQ), and 2,2,2-trifluoroethanol were purchased from Fluka (Taufkirchen, Germany). *N*,*N*-Dimethylformamide (DMF), dichloromethane, and diethyl ether were obtained from Biosolve (Valkenswaard, Netherlands). Acetonitrile was from Merck (Darmstadt, Germany). The following side chain protecting groups were chosen: *tert*-butyl (*t*Bu) for Ser, Thr, and Tyr; *tert*-butyloxy (*t*BuO) for Asp and Glu; trityl (Trt) for Asn, Gln, and His; *tert*-butyloxycarbonyl (Boc) and 1-(4,4-dimethyl-2,6-dioxocyclohex-1-ylidene)ethyl (Dde) for Lys.

The following media and supplements were used for cell cultures: Dulbecco's modified Eagle's medium (DMEM), Ham's F12 (without L-glutamine), RPMI 1640 (with L-glutamine), OptiMEM, HBSS, Dulbecco's phosphate buffered saline (PBS) without calcium and magnesium, foetal calf serum (FCS), L-glutamine, nonessential amino acids, and trypsin/EDTA were obtained from Gibco Life Technologies (Karlsruhe, Germany). Cell culture flasks (75 cm^2) and 24- and 96-well plates were from TPP (Trasadingen, Switzerland). Glass-bottom culture dishes used for confocal and fluorescence microscopy studies were from MatTek Corporation (Ashland, USA). Fluoromount-G was obtained from SouthernBiotech (Birmingham, UK). Lipofectamine 2000, laminin, and GlutaMAX were from Invitrogen (Carlsbad, USA), agarose from Bioline (Berlin, Germany), and the FastRuler DNA ladder High Range was from Fermentas (St. Leon-Rot, Germany). The plasmids pEGFP-N1, pECFP-N1, and pEYFP-N1 (4.733 bp) encoding the enhanced green, cyan, and yellow fluorescent proteins (eGFP, eCFP, eYFP) under the control of the human cytomegalovirus (CMV) immediate early promoter were purchased from Clontech (Mountain View, USA).

Peptide synthesis

The peptides were synthesised according to the Fmoc strategy by using an automated multiple solid-phase peptide synthesiser (Syro, MultiSynTech, Bochum, Germany) as described previously.[64] All peptides were synthesised as C-terminal amides by using the Rink amide resin (0.5 mmol peptide per gram resin). Whereas unlabelled peptides were used for transfection studies, peptide internalisation was performed with N-terminally CF-labelled peptides. The labelling was performed in DMF by using a 1.5-fold excess of CF, DIEA, and HATU while still bound to the resin with fully protected side chains. The overall coupling time was 1 h at room temperature.

The branched peptides were synthesised in two successive SPPS runs. For synthesis of the hCT(9–32) and hCT(18–32) fragments, Fmoc-Lys(Dde)-OH was used to allow selective side chain deprotection at Lys 18 for elongation via the Lys side chain. Accordingly, Fmoc-Lys(Dde)-OH was introduced by double coupling (2×1 h) using a twofold excess of amino acid, HATU, and DIEA. For internalisation studies, the N-terminus of the completed hCT-based fragment was labelled with CF as described above. For N-terminally unmodified branched peptides (required for the transfection studies), the N terminus of the hCT fragment was temporarily protected with Boc (introduced during SPPS as N-terminally Boc-protected amino acid) to avoid side products during the following synthetic steps for peptide branching.

Before Dde deprotection, the CF-labelled hCT fragments were protected by the on-resin introduction of a trityl group as described elsewhere.[65] After the selective removal of the Dde protecting group by using hydrazine in DMF (2% *v*/*v*; 10×10 min at room temperature), the synthesis of the branched peptides was finished via the ε-amino group of Lys 18 in a second SPPS run.

Finally the peptide amides were cleaved from the resins with TFA/thioanisole/thiocresole (90:5:5 *v*/*v*/*v*) within 3 h at room temperature, removing all acid-labile protecting groups simultaneously. After precipitation from and washing (5×) with ice-cold diethyl ether, the peptides were collected by centrifugation, lyophilised from water/*tert*-butyl alcohol (3:1 *v*/*v*), and analysed by analytical RP-HPLC on a Vydac RP C_{18} column (4.6×250 mm; 5 μm/300 Å) using linear gradients of 10–60% B in A (A = 0.1% TFA in water; B = 0.08% TFA in acetonitrile) over 30 min and a flow rate of 0.6 mL min^{-1}. Further purification of the peptides was achieved by preparative HPLC on RP C_{18} column (Waters, 5 μm, 25×300 mm) by using a linear gradient of 20–50% B in A over 50 min and a flow rate of 15 mL min^{-1}. Identification was performed by MALDI-ToF mass spectrometry (Voyager RP, Perseptive Biosystems). Sequences and analytical data are shown in Table 1.

Cell culture

Cells were grown in 75-cm^2 culture flasks to confluency at 37 °C and 5% CO_2 in a humidified atmosphere. HEK 293 cells were cul-

tured in DMEM/Ham's F12 (without L-glutamine) containing 15% heat-inactivated FCS. HeLa cells were grown in supplemented RPMI 1640 (with L-glutamine) with 10% heat-inactivated FCS, MCF-7 cells in DMEM/Ham's F12 (without L-glutamine) containing 10% heat-inactivated FCS and 1% glutamine. SK-N-MC cells were cultured in DMEM (without L-glutamine) containing 10% heat-inactivated FCS, 4 mM glutamine, 1 mM sodium pyruvate, and 0.2% nonessential amino acids. For COS-7 cells, DMEM with 10% heat-inactivated FCS and 1% penicillin/streptomycin was used.

Primary neuron cultures were initiated from rat hippocampi dissociated from 18-day-old foetuses. The dissociation was done by 0.25% trypsin in serum-free HBSS with 0.1% DNase I. Cells were seeded in 12-well plates with cover slips coated with poly-L-lysine and pre-incubated (PBS + 10% FCS). Approximately $25–30\times10^4$ cells were cultured per cover slip in Neurobasal-A medium supplemented with B-27 serum-free supplement (2%) and glutamine (2 mM) at 37 °C and 7% CO_2 in a humidified atmosphere.

Primary chicken cardiomyocytes were isolated from stage-29 (Hamburger Hamilton) *White Leghorn "classic"* embryos. Hearts were excised with two tweezers, and vessels and embryonic connective tissue were removed. The collected hearts were minced into small pieces with scalpel blades and washed with HBSS. The dissociation was done by incubation with 0.25% trypsin/EDTA and 0.3 mg mL^{-1} DNase I, followed by mechanical dissociation with a fire-polished Pasteur pipette. Dissociated cardiomyocytes were resuspended in DMEM with 10% heat-inactivated FCS, 1% GlutaMAX, and 0.2% penicillin/streptomycin. Cells were seeded (40×10^4 per well) in 12-well plates with or without cover slips. Cover slips were pre-incubated with 50 μg mL^{-1} laminin at room temperature overnight.

Resazurin-based cell viability assays

To examine the viability and proliferation by using a resazurin-based in vitro toxicology assay kit, HEK 293 cells were grown to sub-confluency in 96-well plates and then incubated for 24 h under standard growth conditions with up to 150 μM peptide solutions, for 6 h with the transfection mixtures that contain vector DNA and up to 150 μM CQ, and for 4 h with PEI–DNA complexes with N/P ratios of up to 20:1 in OptiMEM.

As negative and positive controls, untreated cells and cells treated for 15 min with 70% EtOH were used. Following incubation, the cells were washed twice with DMEM and subsequently incubated at 37 °C for 2 h with a 10% solution of resazurin in DMEM. Finally, the conversion of resazurin to the reduced resorufin was measured fluorimetrically at 595 nm ($\lambda_{ex}=550$ nm) with a Spectrafluor plus multi-well reader (Tecan, Crailsheim, Germany).

Microscopic studies of peptide uptake

To monitor peptide uptake, unfixed and fixed HEK 293, MCF-7, HeLa, and COS-7 cells as well as primary chicken cardiomyocytes and rat hippocampal neurons were used. Cells were fixed after peptide internalisation by seeding them on cover slips (12 mm) in 12- or 24-well plates. Cells to be studied while living were cultured in glass-bottom culture dishes.

When grown to sub-confluency, the cells were incubated with CF-labelled peptides (concentration range: 5–50 μM) in OptiMEM at 37 °C for 45–90 min. For fluorescence studies on living cells, a Zeiss Axiovert 200 inverted fluorescence microscope with ApoTome was used. The cell nuclei were stained with benzimide H33342 for 10 min prior to the end of the peptide incubation. After incubation, the peptide solution was removed. To quench external CF fluorescence, the cells were treated for 1 min with Trypan blue (6.5 mM in sodium acetate buffer, pH 4.5)[66] and washed three times with PBS (with 0.6% glucose), HBSS, or OptiMEM. For fixation, quenched and washed cells were treated with 4% paraformaldehyde for 30 min. Finally, fixed cells were washed three times for 10 min with PBS (with 0.6% glucose) and embedded with Fluoromount-G.

To counter-stain the cells with transferrin–Texas Red for clathrin-dependent endocytosis, cells were incubated with dye solution (50 μg mL^{-1}) for 2 h prior to and during peptide incubation. The chicken cardiomyocytes were counter-stained histologically with an α-actinin antibody. For this purpose, fixed cells were permeabilised for 60 min with 3% BSA and 0.1% Triton X-100 in PBS. The cells were then incubated with a monoclonal mouse anti-α-actinin antibody for 2 h, washed three times with PBS, and incubated for 90 min with a Cy3-labelled anti-mouse antibody. Untreated cells were used as negative control; cells incubated with 50 μM CF were analysed as reference.

Confocal microscopy studies were carried out with a Leica TCS SP2 AOBS with a PL APO 63×/1.40 oil immersion objective and an Ar laser (100 mW, 488 nm). The investigated cells were treated as described above.

Electromobility shift assays

An EMSA was conducted to determine appropriate peptide–plasmid ratios to ensure complete DNA complexation by the carrier peptides. Therefore, 0.25 μg of the expression vector pECFP-N1 were complexed in four different peptide–plasmid charge ratios (5:1, 15:1, 30:1, and 60:1) with each carrier peptide for 1 h at 37 °C in aqueous solution, followed by gel electrophoresis in 1% agarose. A FastRuler DNA ladder was used as a marker, and pure pECFP-N1 (0.25 μg) was used as control.

Degradation studies in human blood serum

Human blood was taken from a volunteer. After centrifugation, the supernatant was cooled to −80 °C, and samples were used on demand.

The branched hCT-derived peptides hCT(9–32)-2br and hCT(18–32)-k7 as well as the parent peptide hCT(9–32) were dissolved in pre-heated (37 °C) human blood serum to a final concentration of 100 μM in 200 μL, and subsequently incubated for up to 240 h at 37 °C with mechanical shaking (300 rpm). After 1, 6, 12, 24, 48, and 240 h, the samples were mixed with 60 μL acetonitrile/EtOH (1:1 *v/v*) and incubated for at least 6 h at −15 °C for serum protein precipitation. After centrifugation (14000 rpm for 15 min) the supernatant was filtered (pore size: 0.22 μm).

Identification of the fragments was performed by analytical RP-HPLC on a Vydac RP C_{18} column (4.6×250 mm; 5 μm/300 Å) using a linear gradient of 15–60% B in A (A = 0.1% TFA in water; B = 0.08% TFA in acetonitrile) over 30 min, and a flow rate of 0.6 mL min^{-1}. Only the N-terminally labelled fragments were detected by fluorescence emission of CF at 517 nm. The peaks were fractionated, lyophilised and analysed by MALDI-ToF mass spectrometry.

Circular dichroism studies

The CD spectra were recorded with a JASCO model J715 spectropolarimeter over 320–190 nm at 20 °C in a N_2 atmosphere. The CF-labelled peptides were investigated alone and after complexation with the vector DNA pEGFP-N1 in aqueous phosphate buffer (10 mM; pH 7.1). The peptide concentration was 10 μM, and a peptide–plasmid charge ratio of 30:1 was used. For the measurement, a thermostable sample cell with a path length of 0.02 cm was used along with the following parameters: response time, 4 s; scan speed, 50 nm min^{-1}; step resolution, 0.5 nm; and bandwidth, 2 nm. The CD spectra of the buffer and the DNA solution were subtracted from the CD spectra of the peptide and peptide–plasmid complex solutions, respectively, to eliminate the interference from solvent, DNA, and optical equipment. High-frequency noise was decreased by means of a low-path Fourier transform filter. The ellipticity is expressed as molar ellipticity $[\theta]_R$ in deg cm^2 dmol^{-1}.

Peptide-mediated cell transfection with vector DNA

For transfection experiments, cells were grown in 96- or 24-well plates and used when sub-confluent. As vector DNA, pEGFP-N1, pECFP-N1, or pEYFP-N1 (commercially available plasmids of 4.733 bp encoding the enhanced fluorescent proteins) were used. These vectors (0.5–1.5 μg) were complexed for 1 h at 37 °C with the cell-penetrating peptide in aqueous solution using peptide–plasmid charge ratios of 5:1, 15:1, 30:1, and 60:1. In the meantime the cells were pre-incubated for 60 min with OptiMEM in the presence of CQ (0–150 μM). After peptide–plasmid complexation, serum-free OptiMEM and CQ (according to the pre-incubation concentrations) were added to the transfection sample.

The pre-incubation medium was replaced by the transfection sample followed by incubation for 2–4 h under standard growth conditions. Afterward, the mixture was replaced by fresh standard cell culture medium. As negative controls, either untreated cells or cells treated only with plasmid and CQ were used. As positive control, cells were transfected using Lipofectamine 2000 according to the manufacturer's guidelines. After 24 h, the expression of the fluorescent protein was monitored with a Zeiss Axiovert 200 inverted fluorescence microscope (GFP filter: $\lambda_{ex} = 470 \pm 20$ nm, $\lambda_{em} = 525 \pm 25$ nm; CFP filter: $\lambda_{ex} = 436 \pm 10$ nm, $\lambda_{em} = 480 \pm 20$ nm; YFP filter: $\lambda_{ex} = 500 \pm 10$ nm, $\lambda_{em} = 535 \pm 15$ nm).

Finally, to quantify transfection rates and expression levels, cells were trypsinised for 1 min, resuspended in HBSS, and analysed by flow cytometry using a Partec CyFlow ML flow cytometer (at least 10 000 cells per sample).

Abbreviations

bp, base pair; BSA, bovine serum albumin; CD, circular dichroism; CF, 5(6)-carboxyfluorescein; COS-7, African green monkey kidney cell line; CQ, chloroquine; Dde, 1-(4,4-dimethyl-2,6-dioxocyclohex-1-ylidene)ethyl; DEAE, diethylaminoethyl; DIC, diisopropylcarbodiimide; DIEA, *N*,*N*-diisopropylethylamine; DMEM, Dulbecco's modified Eagle's medium; DMF, *N*,*N*-dimethylformamide; eCFP, enhanced cyan fluorescent protein; eGFP, enhanced green fluorescent protein; eYFP, enhanced yellow fluorescent protein; EDTA, ethylenediaminetetraacetic acid; EMSA, electromobility shift assay; EtBr, ethidium bromide; FCS, foetal calf serum; Fmoc, 9-fluorenylmethyloxycarbonyl; HATU, *O*-(7-azabenzotriazol-1-yl)-1,13,3-tetramethyluronium hexafluorophosphate; HBSS, Hank's buffered salt solution; hCT, human calcitonin; HEK 293, human embryonic kidney cell line; HeLa, human cervix carcinoma cell line; HIV-Tat, protein transduction domain derived from human immunodeficiency virus (HIV-1) transactivator of transcription (Tat) protein; HOBt, 1-hydroxybenzotriazole; MALDI-ToF, matrix-assisted laser-desorption ionisation time-of-flight; MCF-7, human breast adenocarcinoma cell line; PBS, phosphate-buffered saline; PEI, polyethyleneimine; RP-HPLC, reversed-phase high-performance liquid chromatography; SK-N-MC, human neuroblastoma cell line; SPPS, solid-phase peptide synthesis; TFA, trifluoroacetic acid; TFE, trifluoroethanol; Trt, triphenylmethyl (trityl).

Acknowledgements

The financial support of the EU by QoL-2001-01451 and of the DFG (SFB 610, TP A1, Z5) is kindly acknowledged. The authors thank R. Reppich for recording the MALDI MS data, A. Faivre for the preparation of rat hippocampal neurons, and M. Schaab for his help in the degradation studies.

Keywords: cell-penetrating peptides · drug delivery · human calcitonin · nucleic acids · primary cells

[1] C. L. Parish, E. Arenas, *Neurodegener. Dis.* **2007**, *4*, 339–347.
[2] J. A. Korecka, J. Verhaagen, E. M. Hol, *Regener. Med.* **2007**, *2*, 425–446.
[3] N. A. Doria-Rose, N. L. Haigwood, *Methods* **2003**, *31*, 207–216.
[4] M. P. Zanin, D. E. Webster, S. L. Wesselingh, *J. Neurovirol.* **2007**, *13*, 284–289.
[5] R. K. Leung, P. A. Whittaker, *Pharmacol. Ther.* **2005**, *107*, 222–239.
[6] G. Liu, F. Wong-Staal, Q. X. Li, *Histol. Histopathol.* **2007**, *22*, 211–217.
[7] P. Y. Lu, F. Xie, M. C. Woodle, *Adv. Genet.* **2005**, *54*, 117–142.
[8] F. Mavilio, G. Pellegrini, S. Ferrari, F. Di Nunzio, E. Di Iorio, A. Recchia, G. Maruggi, G. Ferrari, E. Provasi, C. Bonini, S. Capurro, A. Conti, C. Magnoni, A. Giannetti, M. De Luca, *Nat. Med.* **2006**, *12*, 1397–1402.
[9] C. M. Wiethoff, C. R. Middaugh, *J. Pharm. Sci.* **2003**, *92*, 203–217.
[10] A. Huckriede, J. De Jonge, M. Holtrop, J. Wilschut, *J. Liposome Res.* **2007**, *17*, 39–47.
[11] J. E. Adrian, J. A. Kamps, K. Poelstra, G. L. Scherphof, D. K. Meijer, Y. Kaneda, *J. Drug Targeting* **2007**, *15*, 75–82.
[12] M. Belting, S. Sandgren, A. Wittrup, *Adv. Drug Delivery Rev.* **2005**, *57*, 505–527.
[13] N. S. Yang, J. Burkholder, B. Roberts, B. Martinell, D. McCabe, *Proc. Natl. Acad. Sci. USA* **1990**, *87*, 9568–9572.
[14] T. K. Wong, E. Neumann, *Biochem. Biophys. Res. Commun.* **1982**, *107*, 584–587.
[15] F. L. Graham, A. J. van der Eb, *Virology* **1973**, *52*, 456–467.
[16] R. J. Lee, L. Huang, *Crit. Rev. Ther. Drug Carrier Syst.* **1997**, *14*, 173–206.
[17] N. Maurer, A. Mori, L. Palmer, M. A. Monck, K. W. Mok, B. Mui, Q. F. Akhong, P. R. Cullis, *Mol. Membr. Biol.* **1999**, *16*, 129–140.
[18] D. J. Galbraith, A. S. Tait, A. J. Racher, J. R. Birch, D. C. James, *Biotechnol. Prog.* **2006**, *22*, 753–762.
[19] S. Deshayes, M. C. Morris, G. Divita, F. Heitz, *Cell. Mol. Life Sci.* **2005**, *62*, 1839–1849.
[20] B. Gupta, T. S. Levchenko, V. P. Torchilin, *Adv. Drug Delivery Rev.* **2005**, *57*, 637–651.
[21] A. E. Pontiroli, M. Alberetto, G. Pozza, *Br. Med. J.* **1985**, *290*, 1390–1391.
[22] S. D. Stroop, H. Nakamuta, R. E. Kuestner, E. E. Moore, R. M. Epand, *Endocrinology* **1996**, *137*, 4752–4756.
[23] M. C. Schmidt, B. Rothen-Rutishauser, B. Rist, A. Beck-Sickinger, H. Wunderli-Allenspach, W. Rubas, W. Sadee, H. P. Merkle, *Biochemistry* **1998**, *37*, 16582–16590.
[24] U. Krauss, F. Kratz, A. G. Beck-Sickinger, *J. Mol. Recognit.* **2003**, *16*, 280–287.
[25] Z. Machova, C. Muhle, U. Krauss, R. Tréhin, A. Koch, H. P. Merkle, A. G. Beck-Sickinger, *ChemBioChem* **2002**, *3*, 672–677.
[26] U. Krauss, M. Muller, M. Stahl, A. G. Beck-Sickinger, *Bioorg. Med. Chem. Lett.* **2004**, *14*, 51–54.

[27] C. Foerg, U. Ziegler, J. Fernandez-Carneado, E. Giralt, R. Rennert, A. G. Beck-Sickinger, H. P. Merkle, *Biochemistry* **2005**, *44*, 72–81.
[28] D. Luo, W. M. Saltzman, *Nat. Biotechnol.* **2000**, *18*, 33–37.
[29] R. Rennert, C. Wespe, A. G. Beck-Sickinger, I. Neundorf, *Biochim. Biophys. Acta Biomembr.* **2006**, *1758*, 347–354.
[30] P. Erbacher, A. C. Roche, M. Monsigny, P. Midoux, *Exp. Cell Res.* **1996**, *225*, 186–194.
[31] K. Lundstrom, *Trends Biotechnol.* **2003**, *21*, 117–122.
[32] L. S. Young, P. F. Searle, D. Onion, V. Mautner, *J. Pathol.* **2006**, *208*, 299–318.
[33] C. E. Thomas, A. Ehrhardt, M. A. Kay, *Nat. Rev. Genet.* **2003**, *4*, 346–358.
[34] M. C. Morris, L. Chaloin, J. Mery, F. Heitz, G. Divita, *Nucleic Acids Res.* **1999**, *27*, 3510–3517.
[35] E. Kleemann, M. Neu, N. Jekel, L. Fink, T. Schmehl, T. Gessler, W. Seeger, T. Kissel, *J. Controlled Release* **2005**, *109*, 299–316.
[36] C. Rudolph, C. Plank, J. Lausier, U. Schillinger, R. H. Muller, J. Rosenecker, *J. Biol. Chem.* **2003**, *278*, 11411–11418.
[37] S. Sandgren, F. Cheng, M. Belting, *J. Biol. Chem.* **2002**, *277*, 38877–38883.
[38] J. J. Turner, A. A. Arzumanov, M. J. Gait, *Nucleic Acids Res.* **2005**, *33*, 27–42.
[39] A. Astriab-Fisher, D. Sergueev, M. Fisher, B. R. Shaw, R. L. Juliano, *Pharm. Res.* **2002**, *19*, 744–754.
[40] P. Lundberg, S. El-Andaloussi, T. Sütlü, H. Johansson, Ü. Langel, *FASEB J.* **2007**, *21*, 2664–2671.
[41] F. Simeoni, M. C. Morris, F. Heitz, G. Divita, *Nucleic Acids Res.* **2003**, *31*, 2717–2724.
[42] S. El-Andaloussi, H. J. Johansson, P. Lundberg, Ü. Langel, *J. Gene Med.* **2006**, *8*, 1262–1273.
[43] M. C. Morris, J. Depollier, J. Mery, F. Heitz, G. Divita, *Nat. Biotechnol.* **2001**, *19*, 1173–1176.
[44] S. R. Schwarze, A. Ho, A. Vocero-Akbani, S. F. Dowdy, *Science* **1999**, *285*, 1569–1572.
[45] L. Josephson, C. H. Tung, A. Moore, R. Weissleder, *Bioconjugate Chem.* **1999**, *10*, 186–191.
[46] C. H. Tung, S. Mueller, R. Weissleder, *Bioorg. Med. Chem.* **2002**, *10*, 3609–3614.
[47] S. Futaki, I. Nakase, T. Suzuki, Z. Youjun, Y. Sugiura, *Biochemistry* **2002**, *41*, 7925–7930.
[48] P. E. Thoren, D. Persson, P. Isakson, M. Goksor, A. Onfelt, B. Norden, *Biochem. Biophys. Res. Commun.* **2003**, *307*, 100–107.
[49] M. Hällbrink, A. Florén, A. Elmquist, M. Pooga, T. Bartfai, Ü. Langel, *Biochim. Biophys. Acta Biomembr.* **2001**, *1515*, 101–109.
[50] S. Futaki, *Adv. Drug Delivery Rev.* **2005**, *57*, 547–558.
[51] A. D. Ragin, R. A. Morgan, J. Chmielewski, *Chem. Biol.* **2002**, *9*, 943–948.
[52] M. A. Muñoz-Morris, F. Heitz, G. Divita, M. C. Morris, *Biochem. Biophys. Res. Commun.* **2007**, *355*, 877–882.
[53] E. Gros, S. Deshayes, M. C. Morris, G. Aldrian-Herrada, J. Depollier, F. Heitz, G. Divita, *Biochim. Biophys. Acta Biomembr.* **2006**, *1758*, 384–393.
[54] R. Tréhin, U. Krauss, R. Muff, M. Meinecke, A. G. Beck-Sickinger, H. P. Merkle, *Pharm. Res.* **2004**, *21*, 33–42.
[55] S. Deshayes, A. Heitz, M. C. Morris, P. Charnet, G. Divita, F. Heitz, *Biochemistry* **2004**, *43*, 1449–1457.
[56] M. E. Herbig, U. Fromm, J. Leuenberger, U. Krauss, A. G. Beck-Sickinger, H. P. Merkle, *Biochim. Biophys. Acta Biomembr.* **2005**, *1712*, 197–211.
[57] M. E. Herbig, K. Weller, U. Krauss, A. G. Beck-Sickinger, H. P. Merkle, O. Zerbe, *Biophys. J.* **2005**, *89*, 4056–4066.
[58] K. Wagner, N. Van Mau, S. Boichot, A. V. Kajava, U. Krauss, C. Le Grimellec, A. Beck-Sickinger, F. Heitz, *Biophys. J.* **2004**, *87*, 386–395.
[59] R. Tréhin, H. M. Nielsen, H. G. Jahnke, U. Krauss, A. G. Beck-Sickinger, H. P. Merkle, *Biochem. J.* **2004**, *382*, 945–956.
[60] J. Cheng, R. Zeidan, S. Mishra, A. Liu, S. H. Pun, R. P. Kulkarni, G. S. Jensen, N. C. Bellocq, M. E. Davis, *J. Med. Chem.* **2006**, *49*, 6522–6531.
[61] D. A. Dean, *Exp. Cell Res.* **1997**, *230*, 293–302.
[62] S. Brunner, T. Sauer, S. Carotta, M. Cotten, M. Saltik, E. Wagner, *Gene Ther.* **2000**, *7*, 401–407.
[63] A. Fasbender, J. Zabner, B. G. Zeiher, M. J. Welsh, *Gene Ther.* **1997**, *4*, 1173–1180.
[64] B. Rist, M. Entzeroth, A. G. Beck-Sickinger, *J. Med. Chem.* **1998**, *41*, 117–123.
[65] R. Fischer, O. Mader, G. Jung, R. Brock, *Bioconjugate Chem.* **2003**, *14*, 653–660.
[66] J. Hed, G. Hallden, S. G. Johansson, P. Larsson, *J. Immunol. Methods* **1987**, *101*, 119–125.

Received: August 21, 2007
Revised: December 13, 2007
Published online on January 18, 2008

